JOURNAL OF AIRCRAFT
Vol. 38, No. 1, January–February 2001

Tail Buffet of F/A-18 at High Incidence with Sideslip and Roll (Part 1)

S. Tavoularis* and S. Marineau-Mes†
University of Ottawa, Ottawa, Ontario K1N 6N5, Canada
and
A. Woronko‡ and B. H. K. Lee§
National Research Council, Ottawa, Ontario K1A 0R6, Canada

The unsteady pressure was measured simultaneously at 24 locations on both sides of a vertical fin of a rigid, 6% scale model of the F/A-18 aircraft in a wind tunnel. This pressure was integrated over the entire fin surface and over time to provide the mean and rms normal force, bending moment, and torsional moment on the fin in order to determine its buffet loading. Results are available for Mach numbers $M = 0.25$, 0.60, and 0.80; angles of attack $\alpha = 25$, 30, and 32.5 deg; and a sideslip angle -15 deg $\leq \beta \leq 15$ deg or a roll angle -30 deg $\leq \varphi \leq 30$ deg. At zero roll and sideslip the mean force and moment coefficients generally increased with increasing angle of attack; but as the sideslip or roll angles increased some coefficients changed sign, and their relationships to α became more complex. A measurable trend of the mean force coefficient to decrease with increasing Mach number was also observed. The rms normal force coefficient increased significantly as α increased from 25 to 32.5 deg, but showed no appreciable trends as the Mach number increased from 0.25 to 0.80. The wind-tunnel tests are complemented by a flow-visualization study of the leading-edge extensions vortices of a 1:48 scale model of the F/A-18 in a water tunnel, showing the vortex burst locations at different aircraft orientations. Part 2 of this study presents statistical results of the forces and moments.

Nomenclature

A	=	total fin area
A_j	=	area of jth panel on fin surface
b	=	aircraft span (distance between wing-tip missile launchers)
C_B	=	instantaneous bending moment coefficient about the fin root
C_N	=	instantaneous normal force coefficient
C_T	=	torsion moment coefficient about the quarter-chord line
c	=	wing mean aerodynamic chord (210 mm for the 6% model and 72.9 mm for the 1:48 model)
c_f	=	fin mean aerodynamic chord (128 mm for the 6% model and 44.4 mm for the 1:48 model)
d_c	=	distance of normal force on fin from quarter-chord line
d_{cj}	=	distance of transducer from quarter-chord line
d_r	=	distance of normal force on fin from fin root
d_{rj}	=	distance of transducer from fin root
h	=	vertical fin height from waterline to fin tip
l	=	aircraft length from nose to engine exhaust
M	=	freestream Mach number
p_{Oj}	=	pressure on fin outboard surface at jth panel
p_{Ij}	=	pressure on fin inboard surface at jth panel
q	=	dynamic pressure
Re	=	Reynolds number based on c
x	=	distance from the nose along the axis of the aircraft
y	=	distance from the plane of symmetry of the aircraft
α	=	angle of attack
β	=	sideslip angle
φ	=	roll angle
$\overline{(\cdots)'}$	=	rms value
$\overline{(\cdots)}$	=	mean value

Received 29 February 2000; revision received 19 June 2000; accepted for publication 20 June 2000. Copyright © 2000 by the American Institute of Aeronautics and Astronautics, Inc. All rights reserved.

*Professor, Department of Mechanical Engineering. Member AIAA.
†Research Assistant, Department of Mechanical Engineering.
‡Co-op Student, Institute for Aerospace Research.
§Principal Research Officer, Institute for Aerospace Research. Associate Fellow AIAA.

Introduction

LIKE other high-performance modern fighter aircraft, the F/A-18 was designed to operate under wide ranges of speeds and orientations. It can generate high lift and achieve superior maneuverability at high angles of attack, largely because of its leading-edge extensions (LEX), which are credited with increasing the maximum lift of the aircraft[1] by more than 22% and delaying the angle of maximum lift to as high as 40 deg. These effects have been associated with the pair of LEX vortices, which, at sufficiently large angles of attack, roll up at the LEX edges and are convected downstream. Despite their usefulness, the LEX vortices have also caused concern because they are largely responsible for fatigue failure of the aircraft's aft structures. In particular, at angles of attack above 20 deg the LEX vortices burst upstream of the tail resulting in an unsteady loading of the vertical fins, exciting an aeroelastic response, known as buffeting. Because of the structural damage it causes to the aircraft, buffeting has been the subject of numerous investigations, which include wind-tunnel and water-tunnel studies as well as flight tests.[2–6] An extensive experimental research program has been undertaken by the Institute for Aerospace Research (IAR), using an instrumented, rigid, 6% scale model of the F/A-18 aircraft in IAR's trisonic blowdown wind tunnel. Previously reported results of this program include the pressure fluctuation fields on the LEX and the vertical fin,[7–9] the velocity field in the near wake of the fin,[10] the peak buffet loading of the fin,[11] and the effect of pitch oscillations on vortex bursting and fin buffet.[8] Although the previous publications have documented in detail the interaction between the LEX vortex and the F/A-18's vertical fins and have discussed the effects of Mach number in the subsonic and transonic ranges and the angle of attack, they have not addressed the effect of changing orientation of the aircraft, other than in the pitch direction. This effect is of particular interest because the F/A-18 performs maneuvers with nonzero sideslip and roll angles (see Fig. 1 for angle definitions), although it is known that such orientations substantially alter the aerodynamics of the aircraft and have a significant impact on the LEX vortex structure and path, and, hence, on the vertical fin buffeting.[3] Furthermore, an asymmetric orientation of the aircraft introduces asymmetries in the spanwise flows over the two main wings and differential forces on the vertical tails, which may have

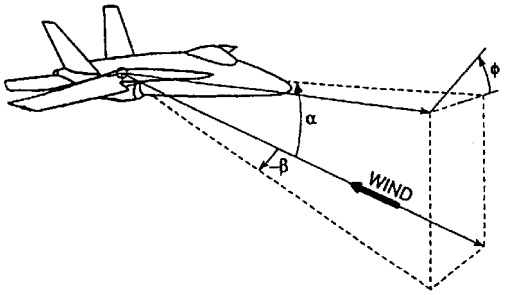

Fig. 1 Definitions of the angle of attack α, the sideslip angle β, and the roll angle φ.

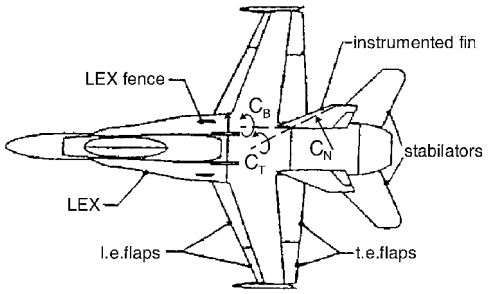

Fig. 2 Sketch of the aircraft model, also showing the positive orientations of the normal force, bending moment, and torsion moment coefficients.

an effect on the lateral and directional stability characteristics of the aircraft. A survey of the available literature revealed only few references that addressed, to a limited extent, the sideslip effect,[3,6,12–16] and, to the best of the authors' knowledge, no references addressed systematically the roll effect. The present research consists mainly of a wind-tunnel study, using the same 6% F/A-18 model, but which was specifically carried out to investigate the effect of sideslip and roll angles on tail buffet at large angles of attack and for different Mach numbers. The present paper is Part 1 of a two-part series, presenting and discussing the high-speed wind-tunnel measurements. It focuses on the mean and rms forces and moments on the vertical fin, whereas Part 2 (Ref. 17) presents a statistical analysis of the pressure distribution on the fin, including two-point correlations and coherence functions between the local pressure and the fin load and spectra of the load. The present paper also reports some flow-visualization results showing the F/A-18 LEX vortex trajectories and burst locations for different values of the angle of attack, the sideslip angle, and the roll angle. These results were obtained using a 1:48 scale model of the F/A-18 in the University of Ottawa water-tunnel facility. Although at a much lower Reynolds number and entirely in the incompressible flow regime, the water-tunnel patterns represent fairly well the actual LEX vortex trajectory and burst locations[3,14,18] and could therefore be useful in interpreting the wind-tunnel results on the loading of the vertical fins at different aircraft orientations.

Experimental Facilities and Measuring Procedures

Wind-Tunnel Tests

These tests were performed in the trisonic blowdown wind tunnel at IAR. A hydraulically driven control system maintained the Mach number constant within ±0.003 while the stagnation pressure was held constant within ±140 Pa. The rigid 6% scale model (Fig. 2) of the F/A-18 aircraft used in this study[7] was fitted with AIM-9 missiles on its wing tips. Its leading-edge and trailing-edge flaps were set at 34 and 0 deg, respectively, and its horizontal stabilators were set at −9 deg, corresponding to the F/A-18 auto flaps-up mode schedule settings at high angles of attack. Boundary-layer transition trips, using rows of epoxy cylinders with diameters of 1.1 mm, separated by 2.5 mm, axis to axis, and 0.05 mm high, were installed 10.1 mm

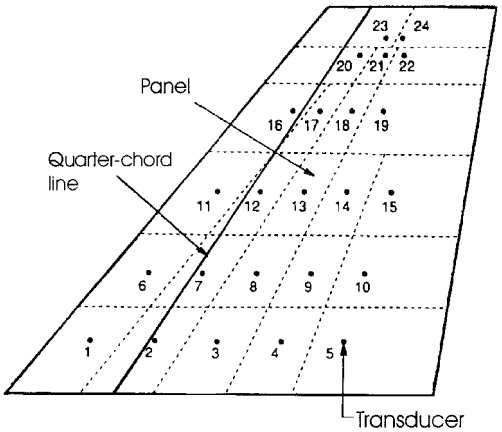

Fig. 3 Locations of pressure transducers on the instrumented fin and area panels used in the computation of the load.

behind the leading edges of the LEX, wings, intakes, vertical tails, and horizontal stabilators on both surfaces.[7] In addition, a ring of the same cylinders was applied around the nose, 10.1 mm behind the tip, and a longitudinal row was fixed on the underfuselage centerline from the nose to the intakes' station.[7] The vertical fins were inclined slightly such that the chord lines formed angles of 1.02 deg with the symmetry plane (with the trailing edges pointing inboard) while the fin centerplanes were tilted (with the tips pointing outboard) by 19.54 deg. Each side of the starboard fin was instrumented with 24 absolute pressure transducers (EndevCO 8515B, 350 kPa full range), embedded under the surface, at the locations shown in Fig. 3. Pressure was sensed via taps, with 0.5 mm diameters and lengths varying from 0.35 to 0.63 mm. Calibration of the transducers was affected by fitting a gas-tight "glove" over the entire fin on the model and subjecting all transducers to a common pressure from a nitrogen supply.[4] The transducer signals were digitized and recorded at a rate of 38,400 samples/s.

The instantaneous normal force coefficient (considered to be positive if the force points in the outboard direction), the instantaneous bending moment coefficient about the fin root (considered to be positive if it deflects the fin tip outboard), and the instantaneous torsion moment coefficient about the quarter-chord line (considered to be positive if it twists the leading edge outboard) were estimated from the following expressions, respectively:

$$C_N = \sum_{j=1}^{24} \frac{(p_{\mathrm{I}j} - p_{\mathrm{O}j})A_j}{qA} \tag{1}$$

$$C_B = \sum_{j=1}^{24} \frac{(p_{\mathrm{I}j} - p_{\mathrm{O}j})A_j d_{\mathrm{r}j}}{qAc_f} \tag{2}$$

$$C_T = \sum_{j=1}^{24} \frac{(p_{\mathrm{I}j} - p_{\mathrm{O}j})A_j d_{\mathrm{c}j}}{qAc_f} \tag{3}$$

where the instantaneous (unsteady) pressures measured by the transducers on the inboard and outboard sides of the fin (Fig. 3) were assumed to be uniform over the corresponding panels. Time series for the instantaneous force and moment coefficients were obtained from the corresponding pressure signals and then processed to provide the mean and rms values. The measured mean force and moment coefficients at zero roll and sideslip were in good agreement with strain gauge measurements of these coefficients on the port fin.[8] Their uncertainty has been discussed in Refs. 8 and 16.

Water-Tunnel Tests

These were performed at the University of Ottawa water tunnel, which is a closed circuit, recirculating flow facility with a test section

0.50 m wide, 0.75 m high, and 4 m long. The plastic model (Revell Monogram F-18C Hornet) was scaled at 1:48. Its leading-edge flaps were set at an angle of 34 deg, whereas the trailing-edge flaps and the horizontal stabilators were kept undeflected at 0 deg. The model was equipped with LEX fences and replicas of AIM 9 wing-tip missiles. Water suction was applied to tubes inserted through the engine exhausts to simulate engine inlet flow, at a speed equal to the freestream velocity. Custom designed mechanisms permitted the pitching, yawing, and rolling of the model, while maintaining the point at $x/l = 0.33$ along the model axis fixed, at a position very close to the center of the water-tunnel cross section. Typical uncertainties in the settings of the different angles were about 0.5 deg. Methyl violet dye was injected through hypodermic tubes, having a 0.39-mm inner diameter and positioned with their tips near the junction of the LEX with the forebody, such that the dye streaks were entrained directly into the LEX vortex core. The dye flow rate was normally adjusted to match the freestream speed of the water, except when enhanced visualization of the tail region was desired, in which case the dye flow rate was doubled. Injection of excess dye appeared to have no noticeable effect on the location of the vortex bursting. Images were recorded using a Sony digital video camcorder. Both plan and side views were taken sequentially at each model orientation. The digital video clips were downloaded onto a PC where they were later manipulated and still images were extracted. The water speed was measured with a two-component, fiber-optic, laser-Doppler velocimeter.

Flow-Visualization Results

General Observations

The reported results were mostly obtained at a freestream velocity of 0.054 m/s, which provided optimum flow visualization of the LEX vortex core. The Reynolds number, based on this velocity and the mean aerodynamic chord c of the model wing, was $Re = 2.66 \times 10^3$. Sample tests at two angles of attack and zero sideslip or roll, conducted at $Re = 2.66 \times 10^3$, 4.04×10^3, 5.43×10^3, and 8.39×10^3, showed variations of the location of vortex bursting by less than 5% of the aircraft length, which is comparable to the uncertainty of observation. Video records of both the plan and side views were obtained for the following model orientations: with the roll angle set at zero, the angle of attack was set at 20, 25, 30, 32.5, or 40 deg; and the sideslip angle was varied between −15 and 15 deg, at steps of 3 deg, for each α; then the sideslip angle was set at zero, the angle of attack was set at 25, 30, or 32.5 deg, and the roll angle was varied between −30 and 30 deg, at steps of 5 deg. Figure 4 is a sample still image, taken from a video clip corresponding to the case with $\alpha = 30$ deg, $\beta = 0$ deg, and $\varphi = -30$ deg; it clearly shows the locations and patterns of LEX vortex bursting for this particular orientation of the model: the leeward vortex remained tight over much of the aircraft's length and burst just before approaching the tail the wing, while the windward vortex burst close to the LEX leading edge. The recorded video clips for different orientations were analyzed by inspection, and the most likely locations of vortex bursting were identified and tabulated. In the absence of sideslip and roll, the two LEX vortices were approximately symmetrical about the model plane of symmetry, whereas introduction of sideslip or roll resulted in asymmetric shifting of both the mean vortex axes and the vortex burst locations. The axial, spanwise, and vertical coordinates of the nominal bursting location, nondimensionalized by the aircraft length l (namely, the distance between the nose and the engine exhaust), half-span $b/2$ (namely, the distance between the plane of symmetry and the wing-tip missile launcher), and fin height h (namely, the distance of the fin tip from the plane containing the nose and the exhaust exit centers "waterline"), respectively, for varying sideslip and varying roll, have been presented in Ref. 19. The presently found streamwise burst locations for zero sideslip and roll at different α compared favorably with corresponding data in water tunnels, wind tunnels, and flight tests,[3] particularly if one considers the appreciable scatter, up to 10% of l, displayed by different tests. Compared to those found in previous water-tunnel tests, the present burst locations, for fixed α and zero sideslip and roll, were

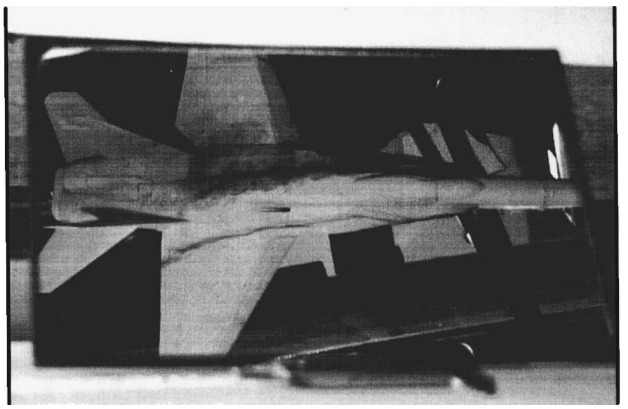

Fig. 4 Water-tunnel flow visualization of the F/A-18 LEX vortices at $\alpha = 30$ deg, $\beta = 0$ deg, and $\varphi = -30$ deg.

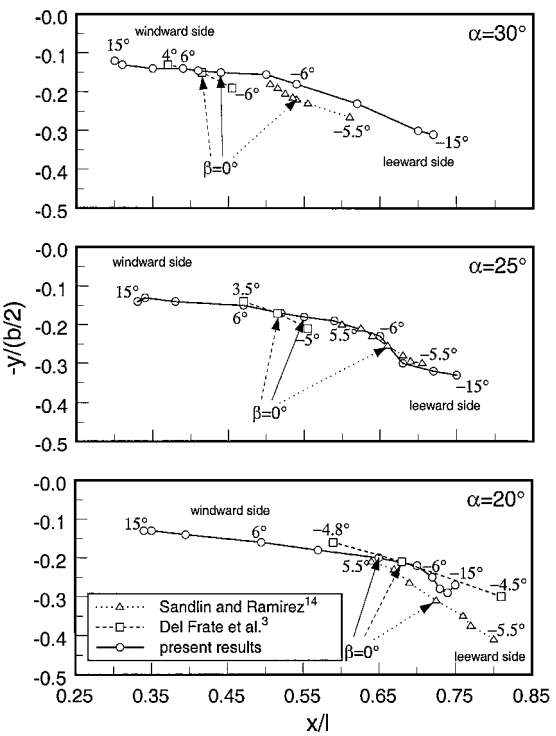

Fig. 5 Variation of the LEX vortex burst location with sideslip angle, based on present and previous[3,14] water-tunnel flow-visualization results.

up to 5% of l downstream of Del Frate et al.'s results[3] and up to 7% of l upstream of Sandlin and Ramirez's results.[14] The latter two references report LEX vortex burst locations for varying sideslip (although for much narrower ranges than those in the present study), although there is no available source reporting similar results for varying roll. It is reminded, however, that any aircraft orientation with respect to the freestream obtained by pitching and rolling is identical to an orientation obtained by pitching and yawing[20] so that it is possible to obtain results with the aircraft in roll by interpolating corresponding results with the aircraft in sideslip.[19]

Effect of Sideslip on Burst Location

The LEX vortex burst locations, on the aircraft planform, for three angles of attack and varying sideslip angle have been summarized in Fig. 5, together with similar results from two other references. The locations corresponding, at least nominally, to the same orientations vary from one experiment to the other, with the present results

being closer to those by Del Frate et al.[3] than those by Sandlin and Ramirez.[14] Besides possible systematic differences in the definitions and determination procedures of the burst locations, discrepancies may have been introduced by small differences in the aircraft model shapes and engine flows, by water-tunnel blockage effects, and by parallax, among others. What is positive, however, when comparing the three sets of results is that one can observe similar trends, as far as the effect of sideslip is concerned: increasing sideslip moved the burst location of the windward vortex toward the LEX apex and the burst location of the leeward vortex toward the tail and away from the plane of symmetry. The present experiments are the only ones for which the sideslip angle extended beyond the ±6-deg range, up to ±15 deg. As shown in Ref. 19, when $\beta > 10$ deg the vortex burst very close to the apex for all five values of α considered, whereas when $\beta < -10$ deg the vortex burst far downstream, near the leading edge of the vertical fin for 20 deg $\leq \alpha \leq$ 32.5 deg or just upstream of the wing leading edge for $\alpha = 40$ deg. With respect to spanwise direction, the burst location on the starboard side remained close to the main wing root for all positive β and moved outboard with increasingly negative β, well surpassing the vertical fin plane; an exception to the latter behavior was the $\alpha = 40^\circ$ case, in which the vortex burst occurred close to the LEX apex for all orientations. The vertical burst location was close to the aircraft's surface at large positive β but remained at a level comparable to the mid-height of the vertical fin at zero and negative β (Ref. 19). In summary, at large positive β, the starboard LEX vortex burst far upstream of the starboard vertical fin, so that the fin was immersed in large-scale, turbulent flow, while, at large negative β, the burst occurred in the vicinity of the fin, towards its outboard side, thus increasing the possibility of large unsteady pressure fluctuations on the fin, especially on its outboard surface.

Effect of Roll on Burst Location

The LEX vortex burst locations, on the aircraft planform, for different angles of attack and varying roll angle have been summarized in Fig. 6. Increasing the roll angle from −30 to 30 deg monotonically shifted the axial location of the starboard LEX vortex burst upstream for all three angles of attack examined. In contrast, the spanwise location changed very little for positive φ and moved outboard for negative φ, while the vertical location moved upward with diminishing positive φ and was nearly constant for negative φ (Ref. 19). A comparison with the corresponding plots with sideslip reveals a prominent similarity in the bursting locations of the LEX vortex under roll with those under sideslip. In both situations a relatively large angle caused the windward vortex to burst near the LEX leading edge and the leeward vortex to burst further downstream. The loci of the burst locations for varying roll show trends comparable to those for varying sideslip, for all three angles of attack for which there are sufficient data. The similarity between the effects of roll and sideslip on the LEX vortex can be attributed to the fact that nonzero roll or sideslip effectively decrease the sweep angle of the windward LEX, while increasing the sweep angle of the leeward LEX, which in both cases results in the same type of asymmetric LEX vortex paths and bursts. These results are to be expected from the equivalence of orientations with pitch and roll and corresponding orientations with pitch and sideslip.[19–22] For example, application of the trigonometric relationships derived in Refs. 19 and 20 shows that the orientation with $\alpha = 30$ deg, $\beta = 0$ deg, and $\varphi = 20$ deg is precisely equivalent to the orientation with $\alpha = 28.48$ deg, $\beta = 9.85$ deg, and $\varphi = 0$ deg, which, for the present rough purposes, can be taken as essentially the same as the orientation with $\alpha = 30$ deg, $\beta = 10$ deg, and $\varphi = 0$ deg. Within the same approximation one can compare the entire $\alpha =$ 30-deg curve for varying sideslip (Fig. 5) with the $\alpha = 30$-deg curve for varying roll (Fig. 6) and see that they are essentially the same, if one uses $\varphi = 2\beta$, which is close to the precise values determined from the equivalence relationship.

The interpretation of the preceding results should be viewed with some caution, in consideration of possible interactions of the LEX vortices with forebody vortices.[23,24] Reference 14 has shown that, for the F/A-18, strong forebody and wing/LEX vortex interactions occur at angles of attack, sideslip, and roll comparable to the ranges used in the present investigation of LEX vortex breakdown. The more powerful LEX vortex attracts the weaker forebody vortex, which is drawn underneath the LEX vortex system. With sideslip the forebody-LEX vortex interactions are such that the windward body vortex is not coupled with the LEX-wing flowfield as strongly as its leeward counterpart (see discussion in the recent review by Lee[25]).

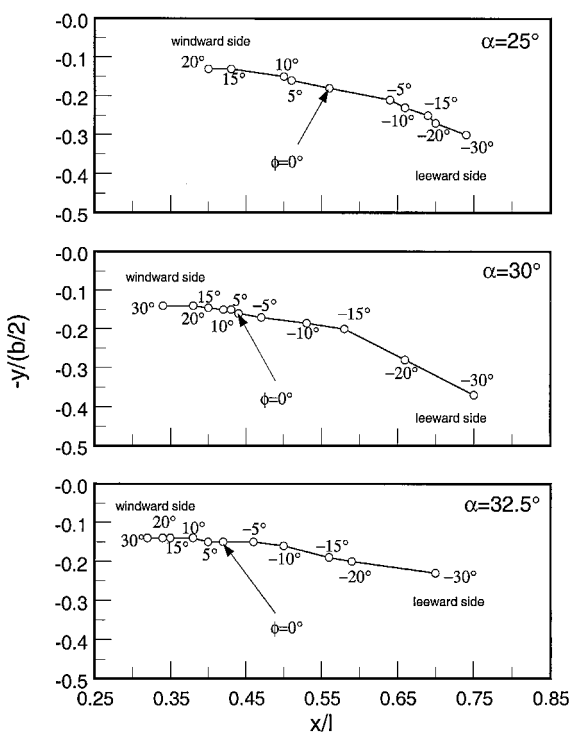

Fig. 6 Variation of the LEX vortex burst location with roll angle, based on present water-tunnel flow-visualization results.

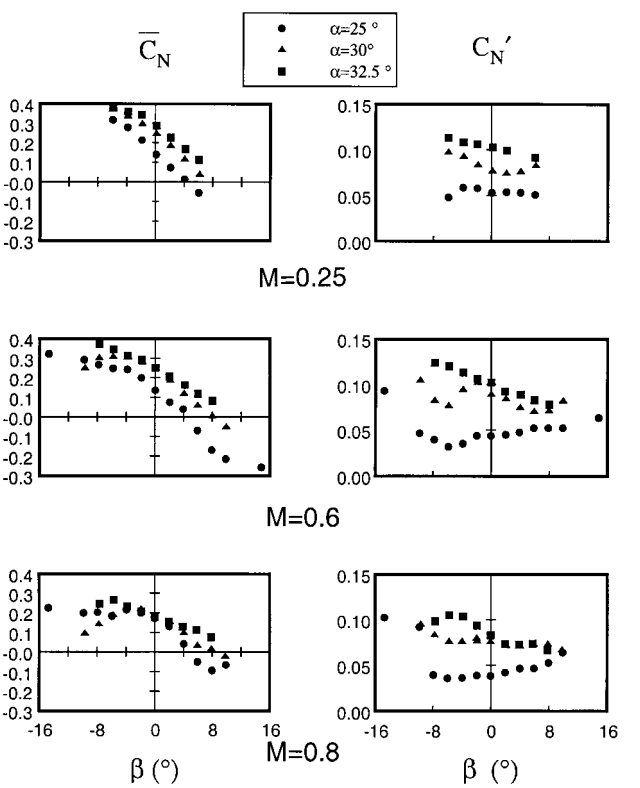

Fig. 7 Effect of angle of attack on the mean and rms normal force coefficients for different Mach numbers and sideslip angles.

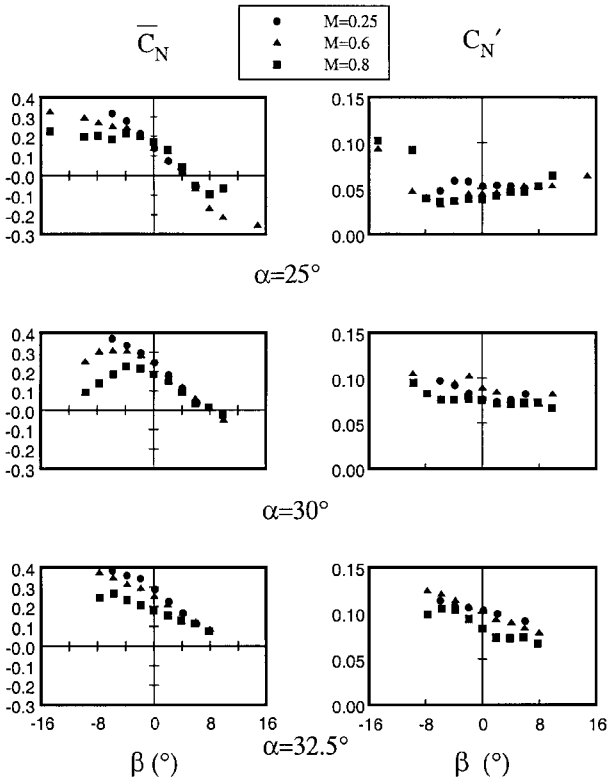

Fig. 8 Effect of Mach number on the mean and rms normal force coefficients for different angles of attack and sideslip angles.

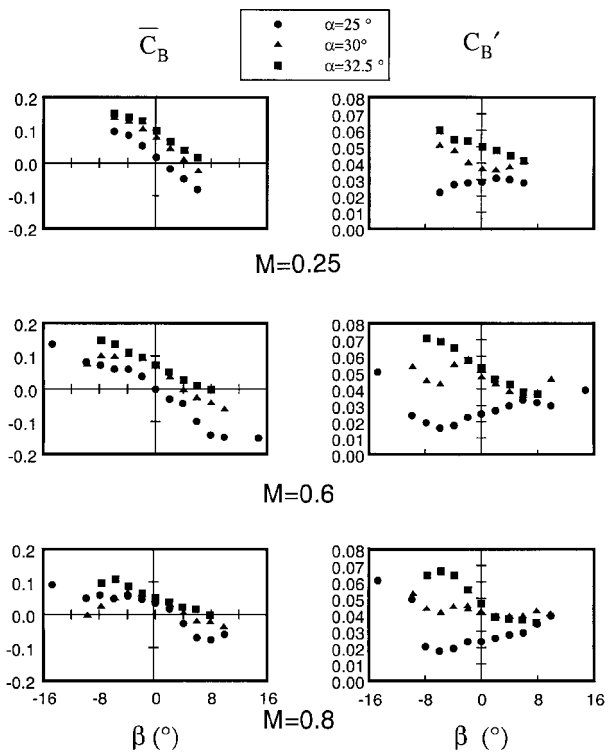

Fig. 9 Variation of the mean and rms bending moment coefficients with sideslip angle.

Wind-Tunnel Measurements

The wind-tunnel measurements are summarized in Figs. 7–11. These measurements include mean and rms values of the normal force coefficient (Figs. 7 and 8), the bending moment coefficient (Fig. 9), and the torsion moment coefficient (Fig. 10) at zero roll and with varying sideslip, for three Mach numbers (0.25, 0.60, and 0.80), and three angles of attack (25, 30, and 32.5 deg), and values of these coefficients at zero sideslip and varying roll for the preceding three Mach numbers but at the single angle of attack of 30 deg (Fig. 11).

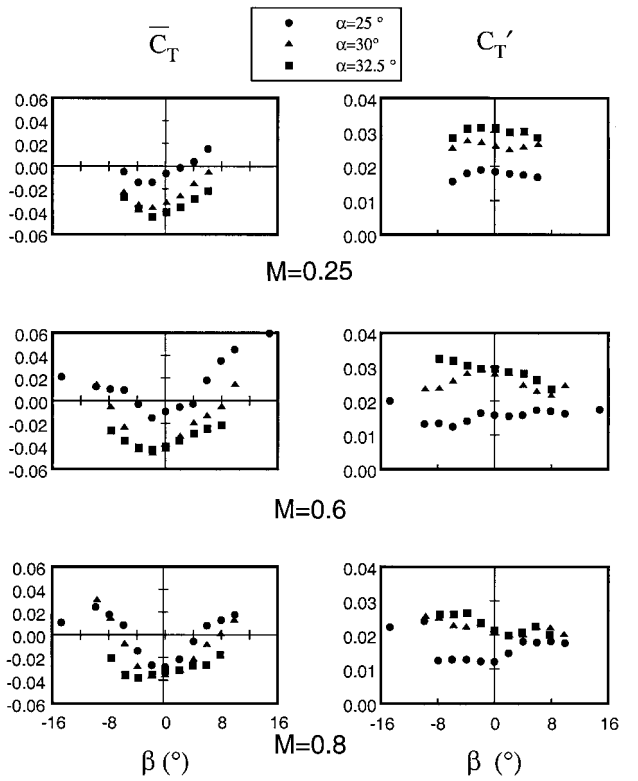

Fig. 10 Variation of the mean and rms torsion moment coefficients with sideslip angle.

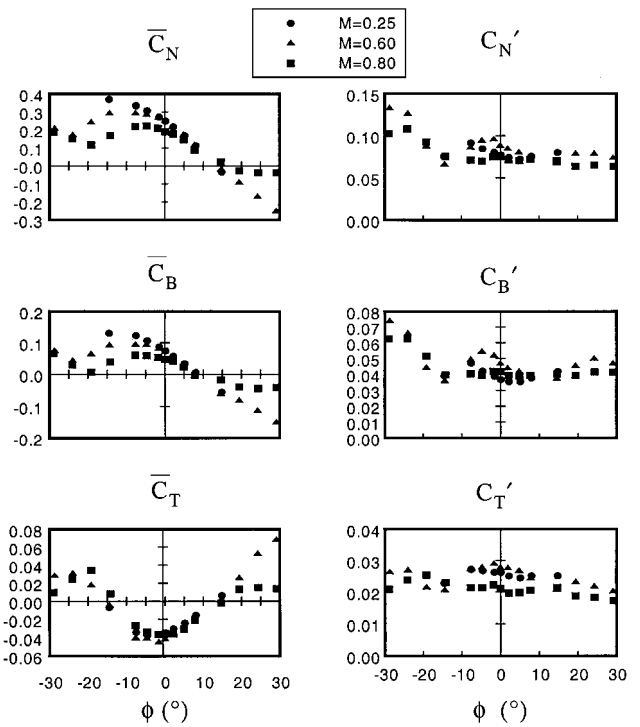

Fig. 11 Variation of the mean and rms force and moment coefficients with roll angle for zero sideslip and α = 30 deg.

Reference Case of Zero Sideslip and Roll

Earlier measurements[7] of $\bar{C}_N$ at $M = 0.60$, for a wide range of α and zero sideslip and roll, show negative loads for $\alpha < 20$ deg and positive loads for $\alpha > 20$ deg, with a maximum value at about $\alpha = 32.5$ deg. The present measurements at symmetric orientations (Fig. 7) are in agreement with the preceding and further show that

for the Mach numbers and angles of attack considered the mean normal force was positive, namely pointing outboard. Total pressure measurements[7,10] of the flowfield just downstream of the fin at $\alpha = 30$ deg have revealed a low pressure, vortical-type region, outboard of the fin. This is clearly caused by the LEX vortex, which, although burst well upstream of the tail at this orientation, it retained an identifiable structure. It has been pointed out[26] that downstream of a spiral vortex breakdown there is a helical flow structure that still generates significant suction, which is not lost entirely until breakdown has reached the apex. Water-tunnel flow visualization at $\alpha = 40$ deg, not achieved in the present wind-tunnel tests, shows that the axes of both vortices passed inboard of the vertical fins[6]; this implies that at sufficiently large α a reversal of the mean force direction can occur. The effect of Mach number on the normal force is shown in Fig. 8. The results follow trends that depend on both M and α but are difficult to generalize. For example, in the $M = 0.25$ tests (Fig. 7) $\bar{C}_N$ increased for α increasing from 25 to 32.5 deg; in the $M = 0.60$ tests $\bar{C}_N$ increased for α increasing from 25 to 30 deg, but was essentially the same for $\alpha = 30$ and 32.5 deg, whereas in the $M = 0.80$ tests $\bar{C}_N$ was nearly the same for the three angles considered. In general, the $M = 0.60$ results are closer to the $M = 0.25$ ones than to the $M = 0.80$ results. Previous literature has identified transonic effects on the LEX vortex at $M = 0.80$: Erickson et al.[2] reported noticeable changes of the shape and position of the LEX vortex, compared to those at lower M, whereas at least for moderate angles of attack there is some evidence for the formation of shock waves over the wing[8] at $M = 0.80$. Therefore, the $M = 0.80$ results should be treated as distinct from those at the lower M. Consistently with the direction of the normal force, the mean bending moment (Fig. 9) about the fin root was also positive, tending to bend the tip outboard. The line of application of this force on the fin can be found by considering that its dimensionless distance from the fin root is given by

$$d_r/c_f = \bar{C}_B/\bar{C}_N \tag{4}$$

The present results show a typical line of application of the normal force at a position, which is about 20% of the fin's height above the root, namely near the boundary between the lowest and the second rows of panels (Fig. 3). The mean torsion moment was negative, tending to twist the leading edge outboard. This means that the mean load applies at a point upstream of the quarter-chord line. The distance of the line of action from the quarter-chord line, found from the expression

$$d_c/c_f = \bar{C}_T/\bar{C}_N \tag{5}$$

was typically 16% of c_f.

In conclusion, it was found that at zero sideslip and roll the normal force applied at a point near the root and the leading edge of the fin, roughly at the boundary between panels 1 and 6, as shown in Fig. 3. Although fin buffeting depends mainly on the load fluctuations, it is reminded that static deformation, caused by steady loading, can also have an effect on the fin's dynamic response, because of the self-induced aerodynamic loads.[27]

The rms force and moment coefficients were all relatively large, with orders of magnitude comparable to those of the corresponding mean coefficients. All values increased significantly with increasing α. The value of C'_T at $\alpha = 32.5$ deg was twice that at $\alpha = 25$ deg. Shah's[6] measurements of the rms bending moment on the vertical fin in essentially incompressible flow also show a sharp increase of this parameter as α increases from about 20 to 38 deg, beyond which it decreased again. The rms load coefficients were only slightly dependent on the Mach number, with the $M = 0.80$ results being somewhat lower than those at lower M. The present results confirm previous findings pointing to the significance of unsteady loading of the vertical fin at large α.

Effect of Sideslip

The sideslip angle was varied by different amounts for each test with a maximum range from -15 to 15 deg. Negative sideslip (see Fig. 1) corresponds to the instrumented fin being on the leeward side, whereas positive sideslip corresponds to the fin being on the windward side. A number of observations can be based on these results, although it is generally clear that the introduction of sideslip greatly complicated the aerodynamic loading of the vertical fin, which, in addition, depended on the angle of attack and the Mach number. The mean normal force and the mean bending moment coefficient decreased almost linearly in the range -4 deg $\leq \beta \leq 4$ deg, for all angles of attack and Mach numbers examined. For larger sideslip angles the trends followed by these parameters depended also on α and M. For example, for $M = 0.60$ (Fig. 7) $\bar{C}_N$ reached a maximum at $\beta \approx -6$ deg when $\alpha = 30$ deg, but it kept increasing with decreasing β within the examined negative sideslip ranges for the other two values of α. Although not always observed within the examined ranges, it is reasonable to postulate that, with increasingly negative β, the mean normal force on the fin would reach a positive peak at some negative β for all α and M. As β increased toward positive values, $\bar{C}_N$ decreased, and, for those tests that contain sufficiently large β results, it crossed zero at a positive β, which seemed to be insensitive to the Mach number (Fig. 8) but increased quite rapidly with increasing α (Fig. 7). Typically, $\bar{C}_N$ crossed zero at $\beta \approx 4$ deg for $\alpha \approx 25$ deg, at $\beta \approx 7.5$ deg for $\alpha \approx 30$ deg, and (by extrapolation) at $\beta \approx 10$ deg for $\alpha \approx 32.5$ deg. At relatively large β of either sign, the normal force magnitude reached maxima, and then it decreased again. It is possible that extensive flow separation over the fin is responsible for this decrease.

The mean bending moment coefficient $\bar{C}_B$ had variations with M, β, and α, which were quite similar to those of $\bar{C}_N$. The values of this coefficient can be used, together with the corresponding values of the load, to estimate the distance of the point of application of the fin load from the fin root, for different sideslip angles. Unfortunately, this procedure becomes increasingly uncertain as the load changes sign, in which case d_r becomes proportional to the ratio of two small numbers. Inspection of the reliable results did not reveal any significant trends, as the distance of the normal force line of action from the fin's root did not seem to shift significantly away from its zero sideslip value. The mean torsion moment coefficient $\bar{C}_T$ had a variation that was quite distinct from those of the other two coefficients, at all examined Mach numbers and angles of attack: it reached a negative minimum at a small negative β (around 2 deg), and it increased to positive values as β deviated from that value. For this coefficient the effect of Mach number appeared to be secondary, whereas the effect of angle of attack was quite measurable with the $\alpha = 30$- and 32.5-deg results being much closer to each other than to the $\alpha = 25$-deg results. Once more, if one excludes the results with near zero load because of their high relative uncertainty, it appears that the point of application of the mean normal force remained between the fin's leading edge and its quarter-chord line throughout the present tests, despite the fact that the direction of the torsion moment changed sign. For a conclusive interpretation of the fin loading patterns, one requires the detailed knowledge of the velocity field around the fin, but, unfortunately, this is not available. Furthermore, flow visualization shows that, under all orientations of present concern, the LEX vortex that interacts with the fin would burst upstream of the fin so that its impact on the fin would be difficult to localize. Consideration, however, of the effective angle of attack of the vertical fin for different sideslip angles makes it clear that moderately negative sideslip would tend to further increase the positive normal force on the starboard fin, whereas positive sideslip would tend to decrease it. For a particular α there is a positive β at which the mean normal force would vanish and beyond which this force would become negative, i.e., inboard. The fact that the zero-force sideslip increases with increasing α while the low-pressure LEX vortex region moves inboard as α increases[3,6] implies that the fin loading depends on the relative position of the LEX vortex axis with respect to the fin for these orientations.

Although the mean loads show some identifiable sensitivity to the dynamic and geometric parameters, the rms load trends are less clear. A general observation is that the rms loads increase substantially with increasing angle of attack at all tested M and β, consistently with the previously documented tail fin buffeting behavior.

The increase can be as high as two- to threefold as α increases from 25 to 32.5 deg. From Fig. 8 the sensitivity of all three coefficients to the Mach number appears not to be strong.

Effect of Roll

All tests at different roll angles were conducted at an angle of attack of 30 deg, zero sideslip, and three Mach numbers 0.25, 0.60, and 0.80, respectively. The roll angle was varied from −30 to 30 deg for the $M = 0.60$ and 0.80 tests, but only from −15 to 15 deg for the $M = 0.25$ tests. Shown in Fig. 11 are the computed mean and rms loads for these tests. As expected by the equivalence between orientations with roll and sideslip, the results shown in Fig. 11 are similar to those presented in the corresponding plots of Figs. 7–10. The variations of $\bar{C}_N$ and $\bar{C}_B$ are strongly asymmetric. In particular, $\bar{C}_N$ increases with increasingly negative φ up to a maximum, which occurred at approximately −5 deg for $M = 0.80$, at −11 deg for $M = 0.60$, and at an angle less than −15 deg for $M = 0.25$, and then it decreases again. At positive roll the $M = 0.60$ results show a monotonic decrease up to $\varphi = 30$ deg, in which case $\bar{C}_N \approx -0.25$, whereas the $M = 0.80$ results reach a plateau at about $\bar{C}_N \approx -0.05$. $\bar{C}_B$ shows a variation that is almost identical to that of $\bar{C}_N$. The variation of $\bar{C}_T$ shows a rather weak dependence on M and a relatively small degree of asymmetry with respect to roll, for $-15 \text{ deg} \leq \varphi \leq 15$ deg, compared to the variations of the other two coefficients. In particular, $\bar{C}_T$ attains its largest, negative, magnitude at a slightly negative roll angle, and then it increases as the roll magnitude increases toward both negative and positive values. It crosses zero at about −15 and 15 deg, and then it attains positive values. The results show that for roll angles in the range from −15 to 15 deg the torsional loading of the vertical tail is such that its leading edge tends to be twisted inward toward the centerplane of the aircraft, whereas for larger roll angles the torsional load has the opposite sense. The general conclusion based on these observations is that the roll angle has a significant effect on the mean loading of the vertical tail fins of the F/A-18. On the other hand, Fig. 11 also shows that the rms values of C_N and C_B have a rather weak sensitivity to Mach number, whereas the rms value of C_T has a stronger dependence on M for $-10 \text{ deg} \leq \varphi \leq 10$ deg.

Conclusions

The present study has contributed new experimental results to the sparse literature on the effects of sideslip and roll on the buffet loads experienced by the vertical fins of the F/A-18 at high angles of attack. The loading patterns that were measured in the wind-tunnel tests have been discussed in the context of new flow-visualization results showing the paths and burst locations of the LEX vortices for ranges of sideslip wider than those reported in previous studies and, for the first time, for wide ranges of roll. Increasing sideslip or roll resulted in a shifting of the burst location of the windward LEX vortex toward the LEX apex and in a shifting of the burst location of the leeward LEX vortex toward the tail and away from the plane of symmetry. For the symmetric orientation of the aircraft, the measured mean force, bending moment, and torsion moment coefficients generally increased with angle of attack increasing from 25 to 32.5 deg and decreased with Mach number increasing from 0.25 to 0.80. The rms normal force coefficient increased significantly with increasing angle of attack but was rather insensitive to Mach-number changes. Subjecting the aircraft to sideslip or roll further increased the complexity of the dependence of the mean coefficients upon α and M, in some cases even reversing the signs of these coefficients for sufficiently large sideslip or roll.

Acknowledgments

Financial support for this project has been provided by the Department of National Defence and by the National Research Council of Canada, Institute for Aerospace Research.

References

[1]Frazier, F. A., "F-18 Hornet—LEX Fence Flight Test Results," *Society of Experimental Test Pilots' Symposium*, Oct. 1988, pp. 72–89.

[2]Erickson, G. E., Hall, R. M., Banks, D. W., Del Frate, J. H., Schreiner, J. H., Hanley, R. J., and Pulley, C. T., "Experimental Investigation of the F/A-18 Vortex Flows at Subsonic Through Transonic Speeds," AIAA Paper 89-2222, July–Aug. 1989.

[3]Del Frate, J. H., Fisher, D. F., and Zuniga, F. A., "In-Flight Flow Visualization with Pressure Measurements at Low Speeds on the NASA F-18 High Alpha Research Vehicle," NASA TM 101726, Oct. 1990.

[4]Lee, B. H. K., Brown, D., Zgela, M., and Poirel, D., "A Wind Tunnel Investigation and Flight Tests of Tail Buffet on the CF-18 Aircraft," *AGARD Conference Proceedings*, CP 483, 1990, pp. 1.1–1.26.

[5]Thompson, D. H., "Water Tunnel Flow Visualization of Vortex Breakdown over the F/A-18," Aeronautical Research Lab., FLIGHT-MECH-R-179, AR-005-607, Melbourne, Australia, Dec. 1990.

[6]Shah, G. H., "Wind Tunnel Investigation of Aerodynamic and Tail Buffet Characteristics of Leading-Edge Extension Modifications to the F/A-18," AIAA Paper 91-2889, 1991.

[7]Lee, B. H. K., and Brown, D., "Wind-Tunnel Studies of F/A-18 Tail Buffet," *Journal of Aircraft*, Vol. 29, No. 1, 1992, pp. 146–152.

[8]Lee, B. H. K., and Tang, F. C., "Unsteady Pressure and Load Measurements on an F/A-18 Vertical Fin," *Journal of Aircraft*, Vol. 30, No. 5, 1993, pp. 756–762.

[9]Lee, B. H. K., and Tang, F. C., "Characteristics of the Surface Pressures on an F/A-18 Vertical Fin due to Buffet," *Journal of Aircraft*, Vol. 31, No. 1, 1994, pp. 228–235.

[10]Lee, B. H. K., Brown, D., Tang, F. C., and Plosenski, M., "Flowfield in the Vicinity of the F/A-18 Vertical Fin at High-Angle-of-Attack," *Journal of Aircraft*, Vol. 30, No. 1, 1993, pp. 69–74.

[11]Lee, B. H. K., and Dunlavy, S., "Statistical Prediction of Maximum Buffet Loads on the F/A-18 Vertical Fin," *Journal of Aircraft*, Vol. 29, No. 4, 1992, pp. 734–736.

[12]Martin, C. A., and Thompson, D. H., "Scale Model Measurements of Fin Buffet Due to Vortex Bursting on F/A-18," AGARD CP-497, May 1991.

[13]Suarez, C. J., and Malcolm, G. N., "Water Tunnel Force and Moment Measurements on an F/A-18," AIAA Paper 94-1802, June 1994.

[14]Sandlin, D. R., and Ramirez, E. J., "A Water Tunnel Flow Visualization Study of the Vortex Flow Structures on the F/A-18 Aircraft," NASA CR 166938, July 1991.

[15]Pettit, C. L., Brown, D. L., Banford, M. P., and Pendleton, E., "Full-Scale Wind-Tunnel Pressure Measurements of an F/A-18 Tail During Buffet," *Journal of Aircraft*, Vol. 33, No. 6, 1996, pp. 1148–1156.

[16]Meyn, L. A., and James, K. D., "Integrated Tail Buffet Loads on the F/A-18," AIAA Paper 94-1801, June 1994.

[17]Tavoularis, S., Marineau-Mes, S., and Lee, B. H. K., "Tail Buffet of the F/A-18 at High Incidence with Sideslip and Roll (Part 2)," *Journal of Aircraft*, Vol. 38, No. 1, pp. 17–21.

[18]Cunningham, A. M., and Bushlow, T., "Steady and Unsteady Force Testing of Fighter Aircraft Models in a Water Tunnel," AIAA Paper 90-2815, 1990.

[19]Tavoularis, S., Marineau-Mes, S., Woronko, A., and Lee, B. H. K., "Unsteady Moments on the F/A-18 Vertical Tail Fin at High Angles of Attack: Effects of Sideslip and Roll," *Proceedings of the 46th Annual CASI Conference*, Canadian Aeronautics and Space Institute, Montreal, Quebec, 1999, pp. 271–281.

[20]Tavoularis, S., "Equivalence Between Sideslip and Roll in Wind Tunnel Testing," *Journal of Aircraft*, Vol. 36, No. 5, 1999, pp. 895, 896.

[21]Ericsson, L. E., "Analysis of the Effect of Sideslip on Delta Wing Roll Trim Characteristics," *Journal of Aircraft*, Vol. 35, No. 5, 1997, pp. 585–591.

[22]Lamont, P. J., and Kennaugh, A., "Total Incidence Plane Aerodynamics: The Key to Understanding High Incidence Flight Dynamics?," *Journal of Aircraft*, Vol. 28, No. 7, 1991, pp. 431–435.

[23]Ericsson, L. E., "Effect of Fuselage Geometry on Delta-Wing Vortex Breakdown," *Journal of Aircraft*, Vol. 35, No. 6, 1998, pp. 898–904.

[24]Ericsson, L. E., "Further Analysis of Fuselage Effects on Delta Wing Aerodynamics," AIAA Paper 2000-0981, 2000.

[25]Lee, B. H. K., "Vertical Tail Buffeting of Fighter Aircraft," *Progress in Aerospace Sciences*, Vol. 36, Nos. 3–4, 2000, pp. 193–279.

[26]Bergmann, B., Hummel, D., and Oelker, H.-Cr., "Vortex Formulation over a Close-Coupled Canard-Wing-Body Configuration in Unsymmetrical Flow," AGARD CP-494, Paper 14, July 1991.

[27]Lee, B. H. K., "A Method for Predicting Wing Response to Buffet Loads," *Journal of Aircraft*, Vol. 21, No. 1, 1984, pp. 85–87.